

Low temperature diamond growth using CO₂/CH₄ plasmas: Molecular beam mass spectrometry and computer simulation investigations

James R. Petherbridge, Paul W. May,^{a)} Sean R. J. Pearce, Keith N. Rosser, and Michael N. R. Ashfold

School of Chemistry, University of Bristol, Bristol, BS8 ITS United Kingdom

(Received 21 August 2000; accepted for publication 23 October 2000)

Microwave plasma enhanced chemical vapor deposition has been used to grow diamond films at substrate temperatures down to 435 °C using CO₂/CH₄ gas mixtures. An Arrhenius plot of growth rate as a function of substrate temperature yields a value for the activation energy for the growth step of 28 kJ mol⁻¹. This is lower than that measured previously for CH₄/H₂ systems and hints at a different gas-surface chemistry when using CH₄/CO₂ plasmas. Molecular beam mass spectrometry has been used to measure simultaneously the concentrations of the dominant gas phase species present during growth, for a wide range of plasma gas mixtures (0%–80% CH₄, balance CO₂). The CHEMKIN computer package has also been used to simulate the experimental results in order to gain insight into the major reactions occurring within the microwave plasma. The calculated trends for all species agree well with the experimental observations. Using these data, the model for the gas phase chemistry can be reduced to only four overall reactions. Our findings suggest that CH₃ radicals are likely to be the key growth species when using CO₂/CH₄ plasmas and provide a qualitative explanation for the narrow concentration window for diamond growth. © 2001 American Institute of Physics. [DOI: 10.1063/1.1333031]

I. INTRODUCTION

The outstanding properties of diamond films grown by chemical vapor deposition (CVD) have attracted much interest during recent years.^{1,2} The now well-established conditions for diamond growth include the use of substrate temperatures >700 °C and a carbon-containing precursor gas diluted in excess hydrogen (typically <5% CH₄ in H₂).³ A major goal in the field of diamond CVD is the lowering of substrate temperatures required for growth, as this could permit the use of a much wider range of substrate materials of industrial importance, such as aluminum, GaAs, nickel, and steel.

Many gas mixtures containing varying ratios of O, C, and H have been investigated in the search for a viable low temperature diamond deposition process. In 1991, Bachmann *et al.*⁴ collated the results from over 70 such deposition experiments to produce an atomic C–H–O phase diagram for diamond deposition (Fig. 1), showing that low pressure synthesis of good quality diamond is only possible within a well defined area close to the H–CO tie line. This indicated that the exact nature of the source gases is unimportant for most diamond CVD processes, and that it is only the relative amounts of C, H, and O which govern whether diamond deposition takes place.

The use of CO₂/CH₄ gas mixtures in microwave plasma CVD (MWCVD) has been reported to enable lower temperature growth.^{5,6} However, the process window for this gas mixture is narrow and centered at a composition of

50% CH₄/50% CO₂ by volume flow rate.^{7,8} Such gas mixtures are unusual in that they contain no input hydrogen, compared to the excess used in other gas mixtures (although the concentration of H₂ in the activated gas mixture is approximately half that seen in CH₄/H₂ mixtures). It has been proposed⁹ that O, O₂, and OH species in the plasma perform some of the roles of the H atoms, such as etching of nondiamond carbon⁷ and the removal of unsaturated hydrocarbons in the gas phase.¹⁰ However, no direct evidence has been presented to support these ideas.

To date, simple optical emission spectroscopy (OES) studies have been the major diagnostic applied to CO₂/CH₄ plasmas.^{7,8,11} Balestrino *et al.*¹¹ found a correlation between optimum diamond growth rate (and quality) and the ratio of the emission intensities from CH (431 nm) and C₂ (505–517 nm) species, and suggested this as a practical gauge to optimize growth conditions for unfamiliar gas mixtures. Mollart and Lewis⁷ found that the ratio of the H_α (656 nm) and C₂ emission peaks varied with gas composition, but that this ratio had only a weak correlation with the diamond deposition domain. OES studies in our own group,⁸ involving a wide range of gas mixing ratios (0%–60% CH₄), showed that maxima in the emission intensity ratios of CH:C₂, H:C₂, and CH:C₃ could all be used as indicators for optimal diamond growth conditions. It was also found that at >55% CH₄ the plasma produced significant amounts of soot, which caused a rising background in the emission spectra at longer wavelengths (>500 nm). This background was attributed to blackbody emission from soot particles in thermal equilibrium with the gases in the plasma region. Fitting this background curve to the Planck distribution function allowed an estimate (2000 K) of the plasma temperature.

^{a)} Author to whom correspondence should be addressed; electronic mail: paul.may@bris.ac.uk

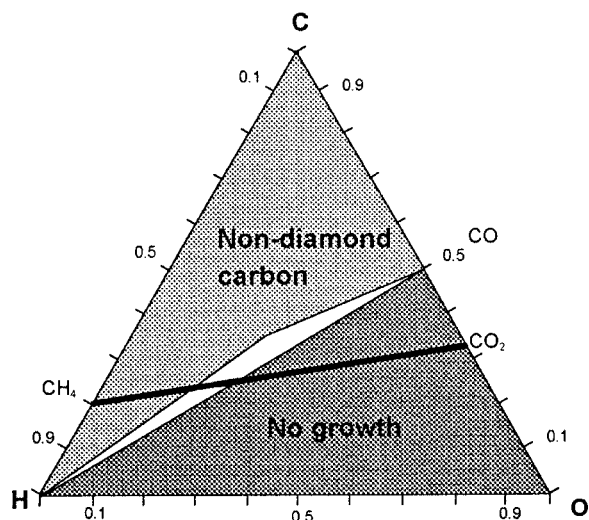


FIG. 1. Simplified atomic C-H-O diamond deposition phase diagram (see Ref. 4). The white area lying above the CO-H tie line is the experimental diamond growth domain. The thick CH₄-CO₂ tie line corresponds to the full range of CO₂/CH₄ gas mixtures used in this work.

However, OES only detects those gas phase species which emit light. In order to understand fully the chemistry of these gas mixtures, measurements of nonemitting species are also necessary. Thus, we have used molecular beam mass spectrometry (MBMS) to detect simultaneously both stable species and more reactive entities, such as radicals. Hsu¹² pioneered the use of MBMS to investigate diamond MWCVD using CH₄/H₂ gas mixtures. In his experiment, the gas was sampled via an orifice in the substrate, allowing analysis of the composition of the flux incident to the diamond growing surface. Later work in our group used MBMS to sample gas directly from the plasma, thus probing the gas phase chemistry in isolation, with minimum perturbation from gas-surface reactions. We have used this powerful technique to obtain absolute mole fractions of the gas phase species present in both hot filament¹³⁻¹⁶ and microwave systems.^{17,18} Itoh and Matsumoto¹⁹ have reported mass spectrometry measurements of CO₂/CH₄ microwave plasmas but in this case MBMS techniques were not used and only a single gas mixture was investigated.

We now report the results of an MBMS study of MWCVD using CO₂/CH₄ gas mixtures over a wide range of plasma compositions (0%–80% CH₄). The measured data have been compared with the results of theoretical modelling of the plasma chemistry using the CHEMKIN suite of computer programs.²⁰ These programs form a comprehensive package that enables the calculation of mole fractions for both stable and unstable species taking part in reactions within the plasma. The calculations evolve from an initial set of starting mole fractions for CO₂ and CH₄. Upwards of 150 reactions involving 28 separate species are then considered simultaneously. Such simulation of CVD growth environments has been carried out previously by our own group^{21,22} and others²³⁻²⁵ for the more familiar gas mixtures, but investigations of CH₄/CO₂ gas mixtures are rare.

II. EXPERIMENT

A. Growth experiments

Diamond deposition was performed using a 1.5 kW ASTeX-style 2.45 GHz microwave plasma CVD reactor. The chamber was water cooled and contained a water-cooled Mo substrate holder. By varying the water flow rate and using steel spacers placed between the cooling coil and the substrate holder, it was possible to achieve and control substrate temperatures in the range 435–845 °C.

The substrate temperature was monitored via a K-type thermocouple clamped into a hole that had been drilled into the underside of the substrate holder (~1 mm from the platen surface). In order for this thermocouple temperature reading to be scaled to give an accurate value of the true temperature of the substrate surface, calibration experiments were performed, the details of which have been reported previously.²⁶

The process gas was a mixture of CH₄ (99.999% purity) and CO₂ (99.99% purity), whose flows were regulated by mass flow controllers. Thus, we define all subsequent gas compositions simply in terms of % CH₄ (= 100 - % CO₂) by flow rate, with total gas flow rate remaining constant at 80 sccm.

Films were deposited on single crystal (100) silicon wafers, manually preabraded with 1–3 μm diamond grit. The duration of deposition was 8 h at a pressure of 40 Torr with 1 kW applied microwave power. All deposition runs reported here used a feedstock gas mixture of 50% CO₂/50% CH₄, while MBMS experiments used gas mixtures containing various ratios of CH₄ and CO₂.

Films were examined using scanning electron microscopy (SEM) to determine crystal morphology and thickness, and by 514.5 nm (Ar⁺) laser Raman spectroscopy to assess film quality.

B. MBMS

A full description of the MBMS system and gas sampling technique has been published previously,^{17,26} but a brief outline will be given here. A two stage differential pumping system was used to sample gas (at 40 Torr) from the side of the microwave plasma ball via an orifice (~100 μm diameter) in a Mo sampling cone. Mo was chosen to be the probe material because other materials either caused excessive soot formation (stainless steel) or etched away (quartz) in the aggressive plasma. Although such an intrusive method is bound to perturb the plasma, the fact that the position of the plasma ball and the reflected microwave power level are insensitive to the presence of the probe, suggest that this perturbation is minimal. Gas passing through this orifice experienced a pressure differential (40–10⁻³ Torr) and underwent adiabatic expansion forming a molecular beam in which chemical reactions were effectively frozen out. The molecular beam then passed through a collimating skimmer into a quadrupole mass spectrometer (Hiden Analytical) maintained at ~10⁻⁶ Torr. Species entering the mass spectrometer were ionized by electron impact. The electron ionization energy is user selectable in the range 4–70 eV. Data reported in this work were recorded with an

electron ionization energy of 18 eV, which is higher than the first ionization potential (IP) of each of the species considered here, i.e., 15.4 (H₂), 9.96 (CH₃), 13.12 (CH₄), 12.67 (H₂O), 11.42 (C₂H₂), 14.1 (CO), and 13.85 eV (CO₂), respectively.²⁷

There are a number of issues to consider in relation to the use of one electron energy for all measurements. First, signal observed at a particular mass to charge (m/z) value could arise from a number of different species. For instance singly charged CO (IP=14.1 eV) and C₂H₄ (IP=10.56 eV) both have $m/z=28$. Thus, measurements for atomic mass 28 were performed at a lower electron energy (13 eV), in order to distinguish between CO and C₂H₄ and verify that the concentration of C₂H₄ was below the experimental detection limits.

Another problem to be considered is that of dissociative ionization. For instance, CH₃⁺ can be formed both by direct ionization of CH₃, and by the dissociative ionization of CH₄ (appearance potential, AP=14.0 eV).²⁸ Thus, a calibration experiment was performed in which CH₄ was introduced into the reaction chamber (in the absence of a plasma) and the $m/z=15$ and 16 signals were monitored, using the standard electron ionization energy of 18 eV. This gave a ratio of CH₃:CH₄ counts of ~0.47, enabling correction of the CH₃ signal measured with the plasma on. The best estimate of the CH₃ signal resulting from direct ionization of CH₃ radicals in the plasma follows the same trend as the "raw" uncorrected data. Other dissociative ionization reactions (e.g., H₂ formation from C₂H₂, H₂O and CH₄, and CO formation from CO₂) all occur at electron energies >20 eV and can therefore be ignored. One other dissociative ionization of possible relevance—the formation of C₂H₂⁺ and H₂ from C₂H₄, AP = 13.1 eV²⁹—is unlikely to be of concern given the low deduced C₂H₄ number densities.

All MBMS measurements were made under the same conditions as the deposition runs, except that the gas mixing ratio was varied and the applied microwave power was increased to 1.2 kW. This is because the presence of the sampling probe reduced the stability of the plasma at 40 Torr, making a higher applied power necessary in order to maintain a stable plasma at this pressure. The temperature of the substrate holder during MBMS measurements varied from ~450 °C for a pure CO₂ plasma to ~400 °C at high % CH₄, for the same flow rate of cooling water.

Compared with our earlier work using CH₄/H₂ plasmas,^{13,17,18} two differences merit note. First, coating (and subsequent charging) of the MBMS source cage results in a medium term drift in ionization efficiency, and therefore signal levels, when using carbon rich process gas (e.g., high % CH₄). It is therefore necessary to measure all the species, at all mixing ratios of interest, in as short a time as possible. In practice, each process gas mixture was allowed to stabilize for ~2 min and the entire mass spectrum ($m/z=0-100$) was then recorded before moving on to the next gas mixture.

Second, it proved impossible to convert the counts measured by the MBMS into absolute mole fractions. This is because, when using CH₄/CO₂ plasmas, it is not possible to provide an absolute calibration for all of the detected species. For this, we would need information about, first, the thermal

diffusion coefficients for species of different masses within the plasma bulk, second, the relative transmission efficiency of the sampling orifice for heavy and light particles, and finally, the detector sensitivity factors for different species. Although estimates for some of these data can be obtained, we lack sufficient information about all of the important species to make conversion of counts into absolute mole fractions reliable. Therefore, no correction has been attempted for these effects, which may result in the experiment being more sensitive to lighter species (e.g., H₂) than heavier species (e.g., CO₂). As a result, no quantitative comparisons of species counts will be made, and the quoted magnitude of signal counts should be treated with caution. Instead, this work will concentrate on comparisons of the trends observed in measured species counts over the range of plasma gas mixtures investigated.

C. Computer simulation

Computer simulations of the gas phase reactions occurring in the microwave plasma were carried out using the SENKIN code, which is part of the CHEMKIN package.^{20,21,25} The relevant H, C, and/or O containing species reactions and temperature dependent rate constants used in the SENKIN calculations were obtained from the GRI-Mech 2.11 reaction mechanism.³⁰ The SENKIN code then calculated equilibrium mole fractions for a fixed reaction mixture (e.g., 50% CO₂/50% CH₄), at a fixed temperature (2000 K) and pressure (40 Torr). Limitations inherent in this approach include:

(1) The plasma is ascribed a single temperature (2000 K). This is a simplification, since in reality the temperature will vary within the plasma ball, being hotter in the center and cooler toward the edges. This is reflected in the visual observations of the plasma, which changes color and brightness from the center outwards.

(2) No electron impact dissociation, ionic reactions, or surface chemistry are included in the modeling. Thus reaction is initiated by thermal dissociation of CH₄ (to give CH₃ and H) and CO₂ (to give CO and O).

(3) No flow of reagents into or out of the reaction volume is considered. To mimic experiment, therefore, it is necessary to run the simulation for a finite time t , only. Simulations were run for $t=1, 2, 3, 4, 5, 10, 20, 30,$ and 300 s. All calculations showed similar trends, with the best agreement with experiment found for $t=5$ s.

III. RESULTS AND DISCUSSION

A. Plasma appearance

The plasma changes in visual appearance with differing CH₄/CO₂ compositions.⁸ 100% CO₂ plasmas appear deep blue with a white center. With additions of <55% CH₄, the plasma does not change significantly in appearance, except that its color becomes a lighter blue. Above 55% CH₄ an orange halo begins to form at the edges of the plasma ball, and the central plasma becomes blue-yellow. Just above the substrate there is a small region ~1 mm wide where the plasma appears violet. The orange halo is believed to be a result of blackbody emission from soot particles that have coalesced in the cooler regions of the plasma.^{8,26} With fur-

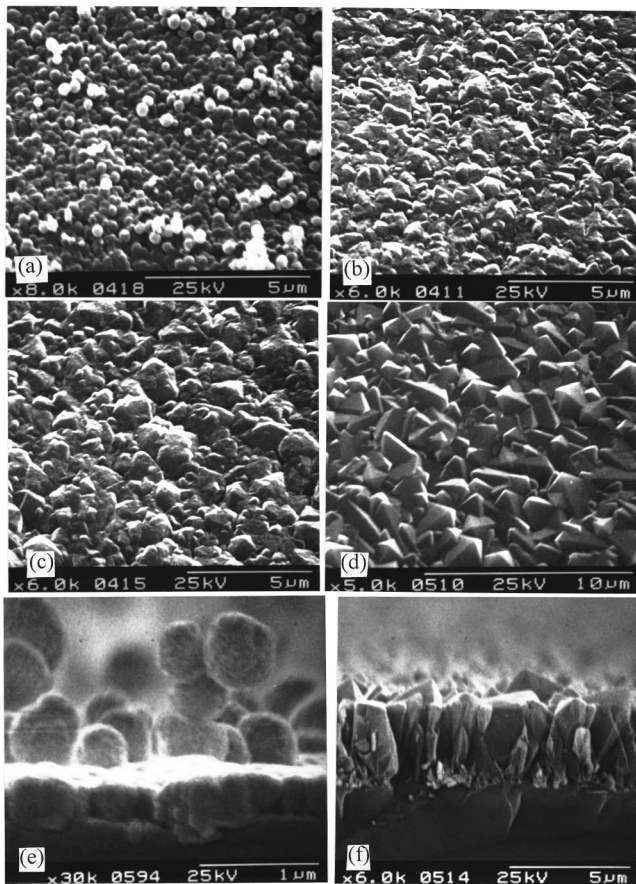


FIG. 2. Electron micrographs illustrating the increase in film crystallinity and facet size obtained with increasing substrate temperature in 50% CH₄/50% CO₂ plasmas. Conditions: 1 kW applied microwave power, total gas flow 80 sccm, pressure 40 Torr, growth time 8 h. Substrate temperature: (a) 435; (b) 590; (c) 650; and (d) 845 °C. Cross sections of two of these films are given in (e) 435 and (f) 845 °C.

ther increases in %CH₄ the orange halo increases in size and brightness, accompanied by rapid deposition of soot on the chamber walls. 100% CH₄ plasmas have a bright white center with an extensive orange halo. Excessive soot deposition at high %CH₄ prevented detailed measurements at these compositions; the MBMS results thus stop at 80% CH₄.

B. Film deposition results

Figure 2 shows the crystallinity and facet size for films grown at various substrate temperatures. At 435 °C (a) the deposit is made up of a barely continuous film of smooth rounded particles. A second layer of isolated rounded particles is beginning to form on top of the first layer, but appears to be poorly adhered. At these low temperatures the temperature difference between the top of the film (closer to the hot plasma) and the bottom of the film (in contact with the cooled substrate) may be sufficient to cause a significant difference in growth rates in the two regions. Thus, deposition occurs faster on top of existing structures, and the deposit grows as rounded isolated pillars. This can clearly be seen in cross section (e), where pillars made from rounded crystallites rise above a smooth continuous coating. At 590 °C (b) and 650 °C (c) a continuous film is obtained, but

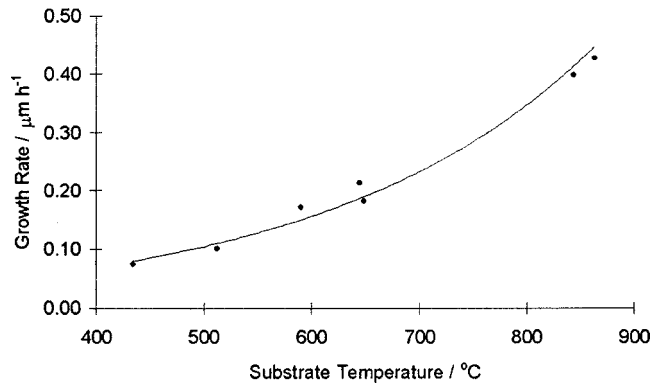


FIG. 3. Film growth rate (measured by cross-sectional SEM) vs substrate temperature for films grown in 50% CO₂/50% CH₄ plasmas. The line is a least squares fit to an exponential function.

with poorly defined crystal facets and small crystal size. The crystallinity improves with increasing substrate temperature, while the number of grain boundaries decreases producing larger crystallites. At 845 °C (d) a continuous film with well-defined, (111) crystalline facets is obtained. The cross section of this film (f) now shows the familiar columnar growth which is characteristic of normal CVD diamond.

Film growth rate is seen to decrease exponentially as the substrate temperature falls (see Fig. 3). At a substrate temperature of 500 °C the growth rate is only 0.1 μm h⁻¹, which must hinder commercial exploitation of these chemistries for low temperature deposition. Figure 4 demonstrates that with decreasing deposition temperature, the full width half maximum (FWHM) of the diamond laser Raman peak at 1332 cm⁻¹ increases, indicating a decrease in the quality of diamond. The height of the diamond peak relative to the graphitic G band at ~1550 cm⁻¹ also decreases with decreasing temperature, reflecting an increase in sp²-bonded carbon content in the films. Since the substrate temperature was controlled independently from other process parameters, the observed decrease in crystallinity, quality and growth rate with lowered substrate temperature is likely to be due to

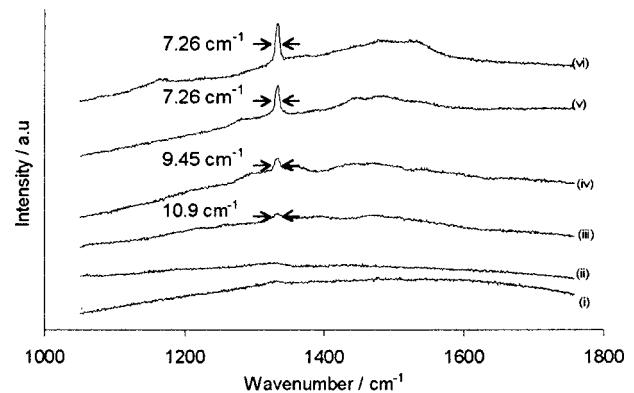


FIG. 4. Laser Raman spectra (514.5 nm excitation) of films grown in a 50% CO₂/50% CH₄ mixture at the following substrate temperatures: (i) 435; (ii) 512; (iii) 590; (iv) 650; (v) 845; and (vi) 865 °C, other conditions as given in Fig. 2. The FWHM values for the diamond peak at 1332 cm⁻¹ are shown on each plot. The spectra have been offset vertically for clarity.

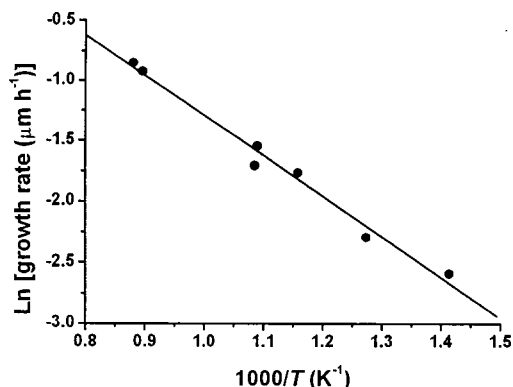


FIG. 5. Arrhenius plot of $\ln(\text{film growth rate})$ vs inverse substrate temperature, $1/T$. The gradient of the fitted line gives an overall activation energy for film deposition of 13 kJ mol^{-1} .

the reduced efficiency of gas-surface and/or surface reaction(s).

An Arrhenius plot for the growth rate data is displayed in Fig. 5. A least squares fit to the data yields a gradient from which an overall activation energy for film deposition of 28 kJ mol^{-1} can be calculated. This activation energy is much lower than the value of 97 kJ mol^{-1} obtained by Kon-doh *et al.*³¹ using a similar analysis of film growth rates obtained using a hot filament CVD reactor and CH_4/H_2 process gas mixtures. In both that report, and the work presented here, the film growth rate was calculated by measuring film thickness by cross-sectional SEM and dividing by the total growth time. However, Snail and Marks³² have pointed out that there is likely to be an (undetermined) nucleation period prior to film growth, and that calculations of activation energy based on such growth rates thus have an inherent un-

certainty. Maeda *et al.*³³ circumvented the problem of an undetermined incubation period by studying changes in the shape of crystals with continued diamond growth (using a 1% CH_4/H_2 microwave plasma) and obtained activation energies of 31 and 84 kJ mol^{-1} for the (100) and (111) crystal planes, respectively. The lower activation energy for CO_2/CH_4 presented here, compared with values from H_2/CH_4 gas mixtures, hints at different fundamental growth steps for these two gas mixtures. It also provides a clue as to why these CO_2/CH_4 plasmas are able to deposit diamond at lower temperatures.

C. MBMS

Figure 6 shows the MBMS counts measured for (i) CO_2 , (ii) CO , (iii) H_2O , (iv) H_2 , (v) CH_3 and CH_4 , and (vi) C_2H_2 , versus the plasma composition. Here it is worth re-emphasising that the relative sensitivity of the mass spectrometer to each species is unknown, and that the relative trends of each specie are the feature of particular interest. Looking at the trends of each specie in turn (with gas mixtures quoted as % CH_4):

(1) **CO_2** : the CO_2 counts fall from an initial high value at 0% CH_4 to zero at 40% CH_4 . This result shows that, even though CO_2 is one of the original input gases, for gas compositions containing more than 40% CH_4 all of this CO_2 is destroyed and converted to other products.

(2) **CO and H_2O** : these follow similar trends, both rising to a peak at $\sim 20\%$ CH_4 , before falling off steadily with further increases in % CH_4 .

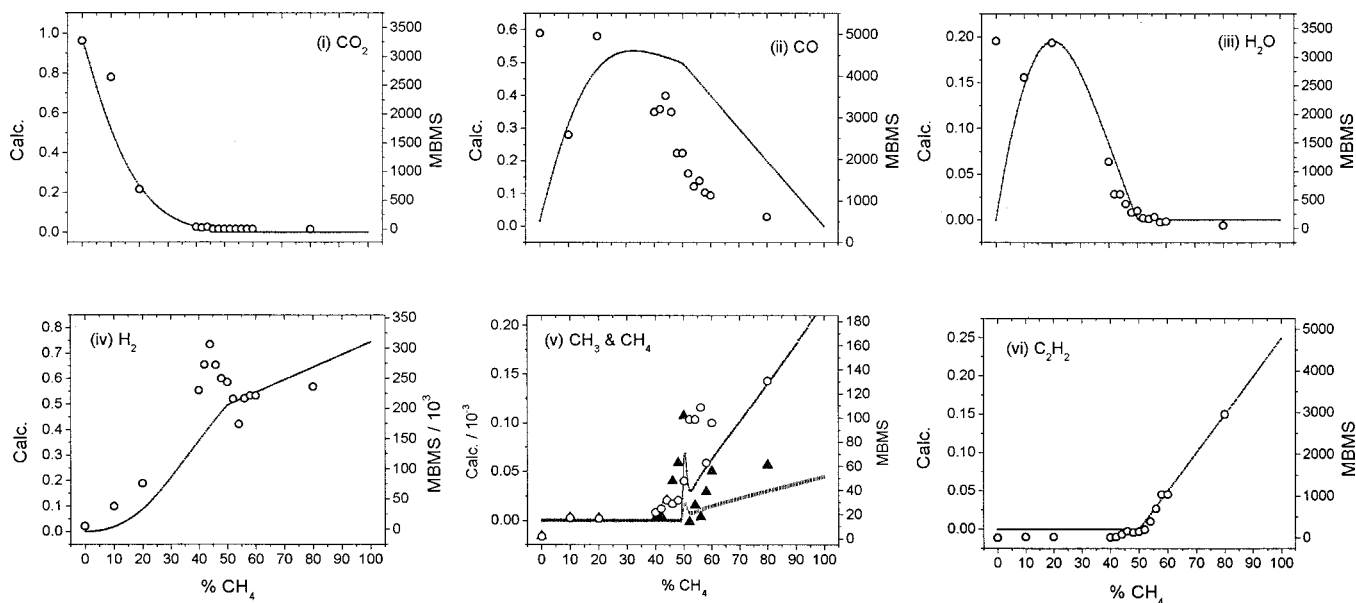


FIG. 6. MBMS plots of species counts (right-hand scale) and SENKIN calculated mole fractions (left-hand scale) vs % CH_4 , in a CO_2/CH_4 gas mixture, for the following species: (i) CO_2 , (ii) CO , (iii) H_2O , (iv) H_2 , (v) CH_3 and CH_4 , and (vi) C_2H_2 . The CH_3 counts are uncorrected for the effect of dissociative ionization of CH_4 , but show the same trend as corrected data. Conditions for MBMS results are as given in Fig. 2, except applied microwave power was increased to 1.2 kW to improve plasma stability. SENKIN computer simulation results are for a CO_2/CH_4 gas mixture at a temperature of 2000 K and a pressure of 40 Torr. Key: \circ MBMS species counts, \bullet SENKIN computer simulation mole fractions, except (v): \blacktriangle MBMS CH_3 counts, ||||| calculated CH_3 mole fractions, \circ MBMS CH_4 counts, \bullet calculated CH_4 mole fractions.

(3) **C₂H₂**: acetylene counts only appear above the background noise for gas mixtures containing over 50% CH₄, but thereafter increase steadily.

(4) **H₂**: the counts for hydrogen rise with increased % CH₄, before leveling out after about 60% CH₄. However, measurements of this light species must be treated with some caution given the large scatter in experimental data.

(5) **CH₃ and CH₄**: counts for CH₃ and CH₄ remain at background levels for low % CH₄ input, and only reach detectable levels above 40% CH₄. This means that for low % CH₄ gas mixtures most, if not all, of the input CH₄ gas is being consumed and converted into other products. At higher % CH₄ mixtures, the curves for both CH₄ and CH₃ rise rapidly to a peak, then fall again over a composition range in which the % CH₄ varies by only ~5%, and thereafter continue rising. The position of the peak is slightly different for the two species: for CH₄ and CH₃ it occurs at 56% and 50% CH₄, respectively. Note that the peak in CH₃ counts coincides very closely with the gas mixture at which the optimum diamond film growth rate and quality is obtained.^{7,8} Note also that the counts of CH₃ and CH₄ are, in general, an order of magnitude lower than those of the other species measured.

(6) **Higher hydrocarbons**: Counts for C₂H₆ or higher hydrocarbons (e.g., C₃, C₄ species, etc.), were not detected, even at very high % CH₄. This is somewhat surprising, given the high levels of soot deposition seen in high % CH₄ plasmas and may, in part at least, be the result of dissociative ionization of the higher hydrocarbons by the 18 eV electrons within the source region of the mass spectrometer. OES and visual inspection suggests that soot formation occurs at the periphery of the plasma, where the gases are cooler. Thus, another explanation may be that no higher hydrocarbons are present in the hotter central region of the plasma, from where the gas is sampled.

(7) **O, O₂, and OH**: counts for these reactive oxygen-containing species are also absent, and it appears that all the oxygen is 'locked-up' within stable molecules, such as H₂O, CO₂, and especially CO. That the concentrations of these reactive species are all below our detection limit encourages the view that they do not play a significant role in the gas phase or surface chemistries, and are therefore not directly involved in the rate limiting processes leading to low temperature diamond growth, contrary to previous suggestions.^{9,10}

D. Computer simulation results and comparison with experiment

Also displayed in Fig. 6 are plots of the relevant species mole fraction versus plasma composition (% CH₄) obtained by computer simulation. The experimental and calculated plots have been scaled vertically to emphasize the remarkable degree of agreement between the two. The falling trend in measured CO₂ counts, and the absence of detectable CO₂ for gas mixtures >45% CH₄ [Fig. 6(i)] are both reproduced by SENKIN simulations. The trends in calculated CO and H₂O mole fractions [Figs. 6(ii) and 7(iii)] are also similar to those observed although rather higher counts of CO and H₂O are seen in experiment at 100% CO₂, where the simulation pre-

dicts zero mole fractions for both species. The presence of CO in the experimental chamber, which is not predicted by the simulation (when using a temperature of 2000 K), may be a result of increased thermal dissociation of CO₂ (to form O and CO) which is found when increased temperatures are used in the simulation. This suggests that the temperature of a pure CO₂ plasma is higher than that for a CO₂/CH₄ plasma (consistent with the increased substrate temperature measured when using a pure CO₂ plasma). This increased temperature for 100% CO₂ might also contribute to the unexpected presence of H₂O counts, by promoting desorption from the chamber walls.

The observed trend in C₂H₂ counts [i.e., a steady rise from zero at ~50% CH₄ gas mixture, Fig. 6(vi)] is also reproduced well by simulation, as are the experimental data for H₂ [Fig. 6 (iv)]. The shape of the curves, trends, and peaks in CH₃ and CH₄ counts are also reproduced well [Fig. 6(v)], although the position of the peak in CH₄ counts is shifted by ~5% between the observed and simulated results.

The simulation also predicts very low mole fractions (<10⁻⁶) for O, OH, O₂, and C₂H₆ (for gas compositions around 50% CH₄, in agreement with the lack of measured counts for these species. The ability of CO₂/CH₄ gas mixtures to enable diamond growth at reduced substrate temperatures (compared to H₂/CH₄ chemistries) is therefore unlikely to be directly due to the presence of O, O₂, or OH in the plasma. Conversely the high levels of CO present in the plasma, found both in experiment and simulation, suggests that CO may be important to the gas-surface chemistry, and therefore to the ability of CO₂/CH₄ gas mixtures to facilitate low temperature growth of diamond.

We note that the very good agreement between experiment and simulation for these gas mixtures (especially over the range of plasma compositions used for diamond deposition, 45%–55% CH₄) arises without including electron impact dissociation or any ionic reactions. Such a finding serves to reinforce previous suggestions¹² that these reactions do not constitute a significant part of the plasma chemistry in typical low pressure MWCVD reactors.

IV. DISCUSSION

Comparing growth rate data at different substrate temperatures for CH₄/H₂ and CH₄/CO₂ gas mixtures, some insight into the growth mechanisms can be deduced. Creation of a dangling bond by abstraction of a hydrogen atom from the diamond surface by reactive gas phase H atoms is generally considered to be a key part of the rate limiting step in the growth mechanism from H₂/CH₄ gas mixtures. The activation energy for diamond growth using 1% CH₄/H₂ gas mixtures has been measured by Kondoh *et al.*³¹ as 97 kJ mol⁻¹ and by Maeda *et al.*³³ as 31 and 84 kJ mol⁻¹ for the (100) and (111) crystal planes, respectively. In the present work, Fig. 5 suggests an activation energy for CH₄/CO₂ plasmas of only 28 kJ mol⁻¹. This lower value suggests that there are fundamental differences in the rate limiting growth step for diamond CVD using these two gas systems.

TABLE I. Species mole fraction results from SENKIN simulations of 1% CH₄/H₂ and 50% CO₂/50% CO₂ gas mixtures. Conditions: temperature 2000 K, pressure 40 Torr.

Species	Mole fraction 50% CO ₂ /50% CH ₄	Mole fraction 1% CH ₄ /H ₂
O	1.11×10^{-8}	0
O ₂	1.53×10^{-11}	0
OH	1.59×10^{-6}	0
CO ₂	3.49×10^{-4}	0
CO	4.97×10^{-1}	0
H ₂ O	1.58×10^{-3}	0
H	4.91×10^{-3}	6.98×10^{-3}
H ₂	4.95×10^{-1}	9.88×10^{-1}
CH ₄	6.61×10^{-5}	4.80×10^{-5}
CH ₃	1.62×10^{-5}	8.36×10^{-6}
C ₂ H ₂	9.22×10^{-4}	4.90×10^{-3}
C ₂ H ₄	1.57×10^{-7}	1.58×10^{-6}
C ₂ H ₆	1.03×10^{-10}	4.14×10^{-11}

Table I shows that under optimal growth conditions (50% CH₄), species such as O, O₂, and OH are present in amounts that are too small to account for a significant change in growth chemistry. We note that the gas phase concentration of CO within the CO₂/CH₄ plasma is ~ 100 times that of atomic H (see Table I). Thus, CO must be considered as an alternative species that could terminate the growing diamond surface. Although a CO-terminated structure is possible, since it involves an unpaired electron it is likely to be rather unstable, and the CO would be expected to readily desorb. A more stable surface termination would occur if the terminating species were CHO (formyl radical), as shown in Fig. 7. This could be formed by direct abstraction of an H (with the excess energy dissipated within the lattice) or by abstracting a neighboring surface terminating H atom. This latter process is attractive in that it provides a means by which the “dangling bond” can migrate across the growing diamond surface (e.g., to a step edge).

We can obtain insight into the thermodynamics of such systems by approximating the structure of the CHO and H-terminated diamond surfaces as tertiary butyl fragments bonded to either CHO or H leaving groups. Thus, we wish to compare the (CH₃)₃C–H bond energy of tertiary butane with the (CH₃)₃C–CHO bond energy of 2,2-dimethylpropanal.

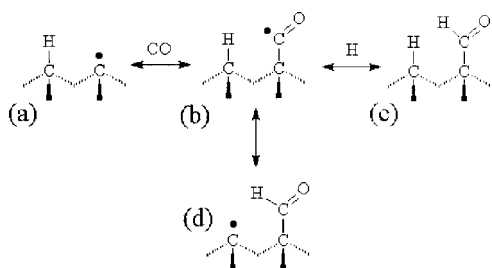


FIG. 7. A model for the behavior of CO on a diamond surface. (a) a reactive site on the diamond surface (the unpaired electron indicated by a dot) reacts with a gas phase CO molecule to form an unstable carbonyl radical adduct, (b). This adduct will most likely rapidly desorb back to (a), although another possibility is that it can be temporarily stabilized by addition of H to form an aldehyde. The H atom could be from the gas phase (c), or a terminating H atom from a neighboring surface site (d).

The bond energy of the former is known from standard tables³⁴ to be -390 kJ mol^{-1} . The relevant C–C bond energy for the latter can be estimated by summing the enthalpies of formation of its component parts, following the method given in Ref. 35. This calculation gives a value for the standard enthalpy of formation of gaseous (CH₃)₃CCHO of $\sim -244 \text{ kJ mol}^{-1}$, which compares favorably with the known enthalpies for similar molecules, such as *n*-pentanal ($-228.5 \text{ kJ mol}^{-1}$) and butan-2-one ($-262.5 \text{ kJ mol}^{-1}$). Since the standard enthalpies of formation of the (CH₃)₃C and CHO radicals are known³⁴ to be $+37.8 \text{ kJ mol}^{-1}$ each, then Hess's law gives an estimate for the relevant C–C bond energy in (CH₃)₃C–CHO as -320 kJ mol^{-1} , some 70 kJ mol^{-1} weaker than the H-terminated structure. Thus, we envisage a more dynamic surface chemistry than with the traditional CH₄/H₂ gas mixtures, involving frequent attachment and detachment of CO molecules to and from the surface, some stabilization of these CO molecules as HCO adducts, and enhanced opportunity for site migration.

Itoh and Matsumoto¹⁹ used x-ray photoelectron spectroscopy to identify adsorbed CO molecules on the surface of deposits obtained from a CO₂/CH₄ microwave plasma. They went on to speculate that CO may be a growth species when using such gas mixtures. However, Eaton and Sunkara³⁶ concluded that although CO species are dominant in the gas phase chemistry they do not participate in gas-surface chemistry. Such contradictions highlight the lack of knowledge of gas-surface chemistry occurring during CVD growth using CO₂/CH₄ gas mixtures.

We turn now to the question of the growth species. In CH₄/H₂ gas mixtures, the growth species are believed to be methyl radicals, which react with dangling bonds on the surface, so adding a carbon to the lattice. In CH₄/CO₂ mixtures, the peak in CH₃ observed both in experiment and simulation coincides very precisely with the narrow window for optimum diamond deposition (50% CO₂/50% CH₄). The fact that there is no similar maximum in the concentration of CO (nor any other species) around this narrow concentration window, provides strong evidence that CH₃ is the species responsible for diamond growth, rather than CO or C₂H₂.

The trends observed in the measured counts of CO₂, CO, and H₂ (i.e., with increasing % CH₄ the CO₂ counts fall while CO and H₂ counts rise) can be explained in terms of the overall reaction scheme 1. Note that this “overall” reaction is actually the net result of a sequence of 12 elementary reactions involving atoms, radicals and molecular fragments



The values for the enthalpy, ΔH , the entropy, ΔS , and the Gibbs free energy, ΔG , for reaction (1) at 2000 K are 251, 0.279, and -306 kJ mol^{-1} , respectively.³⁷ The high negative value for ΔG shows that this reaction occurs spontaneously at these temperatures and that the equilibrium lies far to the right hand side (with equilibrium constant, $K_{\text{eq}} \sim 10^8$, obtained using the relationship $\Delta G = -RT \ln K$). Note that there is a 1:1 stoichiometric relationship between the two reactants, CO₂ and CH₄. This means that each CO₂ molecule

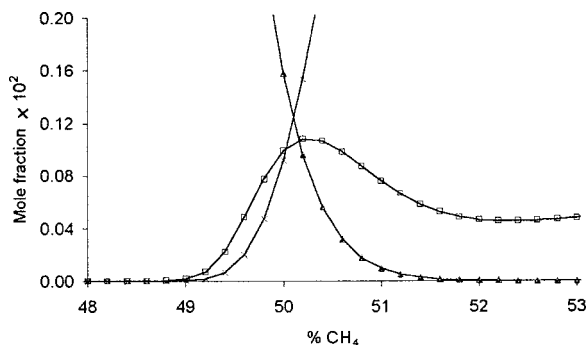


FIG. 8. Calculated species mole fractions close to the 50% CH₄ region, showing H₂O concentrations falling and C₂H₂ concentrations increasing. The species concentrations are equal at approximately the position where CH₄ concentration peaks. The data for CH₄ have been multiplied by a factor of 15 to fit onto the vertical scale. Key: Δ H₂O, \times C₂H₂, \square CH₄.

will react with and “destroy” a CH₄ molecule, but as soon as there is an excess of either of the reactants, that reactant will then be able to undergo further reactions. Therefore, at compositions <50% CH₄, reaction (1) is responsible for the destruction of *all* CH₄ and therefore the suppression of C₂H₂ formation via overall reaction (2). The excess CO₂ is converted into CO and water. Above 50% CH₄ there is now an excess of CH₄, so that not all CH₄ is destroyed in reaction (1). Unreacted CH₄ is thus available to react to form C₂H₂ [reaction (2)], thus explaining why C₂H₂ is only observed at compositions <50% CH₄. Such trends, and their sensitivity to the relative partial pressures of CH₄ and CO₂, reinforce the general discussion of diamond CVD using H/C/O gas mixtures as reviewed by Goodwin and Butler.³⁸

The observed trend in measured counts of H₂O (i.e., peaking at 20% CH₄ before falling to zero at 50% CH₄) can be explained by overall reaction (3). The values of ΔH , ΔS , and ΔG for this reaction at 2000 K are 26, 0.026, and -25 kJ mol^{-1} , respectively.³⁷ Again, the negative value of ΔG shows that this reaction occurs spontaneously at these temperatures and that the equilibrium favours the products ($K_{\text{eq}}=5$). Thus, this reaction serves to reinforce reaction (1), reducing CO₂ to CO with concomitant conversion of H₂ to water



The local peak in CH₄ concentration at 50% CO₂/50% CH₄, seen both experimentally and in simulation, coincides with the composition where the product of the C₂H₂ and H₂O concentrations is a maximum (see Fig. 8). This suggests that this peak in CH₄ concentration is due to an overall reaction between C₂H₂ and H₂O, such as the following reaction:



The values for ΔH , ΔS , and ΔG for this reaction at 2000 K are -180 , -0.022 , and -137 kJ mol^{-1} , respectively.³⁷ ΔG is again large and negative, showing that this reaction occurs spontaneously at these temperatures, and that the equilibrium lies well over to the right-hand side ($K_{\text{eq}}=3700$). At higher % CH₄, the CH₄ concentration is in equilibrium with that of C₂H₂ via reaction (2). The peak in CH₄ (and also CH₃) concentration around 50% CH₄ can now

be seen as the result of competition between two reactions, which begin to contribute and to oppose each other as soon as there is more CH₄ than CO₂. With increasing % CH₄, there is less CO₂ present in the plasma, and as this is a reactant in reaction (3), less product (H₂O) is formed. Thus, the concentration of H₂O falls. But at the same time, increasing % CH₄ increases the amount of C₂H₂ present [reaction (2)]. So, in reaction (4), as the % CH₄ is increased one reactant (H₂O) is decreasing in concentration whilst the other (C₂H₂) is increasing. The concentration where the 1:1 stoichiometry occurs for maximum yield (i.e., maximum CH₄ product) is where the two curves cross, at 50%–51% CH₄. This small window where the CH₃ concentration is maximized, with minimal C₂H₂ present, is the diamond growth window. At even higher CH₄% there is more total CH₃ present, but this is swamped by the excess of C₂H₂, with the result that, as in the traditional CH₄/H₂ chemistry, the deposited films become increasingly graphitic in nature.

V. CONCLUSIONS

CO₂/CH₄ microwave plasmas show promise for the deposition of diamond films at lower substrate temperatures than is possible with traditional CH₄/H₂ chemistries. Detailed investigations of plasma composition using MBMS techniques have provided new insight into the fundamental chemistry occurring in the gas phase and possible clues as to the gas-substrate surface chemistry. A mechanistic explanation for these experimental results has been obtained by comparison of the experimental data with computer simulation of the plasma chemistry. Results suggest that when CO₂/CH₄ gas mixtures are used CO might be involved in the surface termination of the growing diamond film and also that CH₃ is a diamond growth species. Further work will involve probing the plasma chemistry by absorption spectroscopy and more detailed computer modeling of the gas phase reactions.

ACKNOWLEDGMENTS

The authors would like to thank the EPSRC for project funding and De Beers Industrial Diamond, Ltd. for financial support (JRP). Thanks also go to Dr. C. M. Western, Professor R. W. Alder, J. M. Hayes, L. Corbin, T. P. Mollart, and M. A. Elliott for their many and varied contributions to aspects of this work. We also wish to thank Evaldo Corat of the INPE, Brazil, for helpful discussions and suggestions.

¹K. E. Spear, J. P. Dismukes, *Synthetic Diamond, Emerging CVD Science and Technology* (Wiley, New York, 1994).

²P. W. May, *Philos. Trans. R. Soc. London, Ser. A* **358**, 473 (2000).

³*Low-Pressure Synthetic Diamond*, edited by B. Dischler and C. Wild (Springer, Berlin, 1998).

⁴P. K. Bachmann, D. Leers, H. Lydtin, and D. U. Wiechert, *Diamond Relat. Mater.* **1**, 1 (1991); P. K. Bachmann, H. G. Hagemann, H. Lade, D. Leers, F. Picht, and D. U. Wiechert, *Mater. Res. Soc. Symp. Proc.* **339**, 267 (1994).

⁵C. F. Chen, S. H. Chen, H. W. Ko, and S. E. Hsu, *Diamond Relat. Mater.* **3**, 443 (1994).

⁶J. Stiegler, T. Lang, M. Nygard-Ferguson, Y. von Kaenel, and E. Blank, *Diamond Relat. Mater.* **5**, 226 (1996).

- ⁷T. P. Mollart and K. L. Lewis, *Diamond Relat. Mater.* **8**, 236 (1999).
- ⁸M. A. Elliott, P. W. May, J. Petherbridge, S. M. Leeds, M. N. R. Ashfold, and W. N. Wang, *Diamond Relat. Mater.* **9**, 311 (2000).
- ⁹Y. Muranaka, H. Yamashita, K. Sato, and H. Miyadera, *J. Appl. Phys.* **67**, 6247 (1990).
- ¹⁰T. Kawato and K. Kondo, *Jpn. J. Appl. Phys., Part 1* **26**, 1429 (1987).
- ¹¹G. Balestrino, M. Marinelli, E. Milani, A. Paoletti, I. Pinter, A. Tebano, and P. Paroli, *Appl. Phys. Lett.* **6**, 879 (1993).
- ¹²W. L. Hsu, *J. Appl. Phys.* **72**, 3102 (1992).
- ¹³C. A. Rego, P. W. May, C. R. Henderson, M. N. R. Ashfold, K. N. Rosser, and N. M. Everitt, *Diamond Relat. Mater.* **4**, 770 (1995).
- ¹⁴R. S. Tsang, C. A. Rego, P. W. May, J. Thumin, M. N. R. Ashfold, K. N. Rosser, C. M. Younes, and M. J. Holt, *Diamond Relat. Mater.* **5**, 359 (1996).
- ¹⁵C. A. Rego, R. S. Tsang, P. W. May, M. N. R. Ashfold, and K. N. Rosser, *J. Appl. Phys.* **79**, 7264 (1995).
- ¹⁶R. S. Tsang, P. W. May, M. N. R. Ashfold, and K. N. Rosser, *Diamond Relat. Mater.* **7**, 1651 (1998).
- ¹⁷S. M. Leeds, P. W. May, E. Bartlett, M. N. R. Ashfold, and K. N. Rosser, *Diamond Relat. Mater.* **8**, 1377 (1999).
- ¹⁸S. M. Leeds, P. W. May, M. N. R. Ashfold, and K. N. Rosser, *Diamond Relat. Mater.* **8**, 226 (1999).
- ¹⁹K. Itoh and O. Matsumoto, *Thin Solid Films* **316**, 18 (1998).
- ²⁰R. J. Kee, F. M. Rupley, and J. A. Miller, Sandia National Laboratories Report SAND89-8009B (1989).
- ²¹R. S. Tsang, P. W. May, J. Cole, and M. N. R. Ashfold, *Diamond Relat. Mater.* **8**, 1388 (1999).
- ²²R. S. Tsang, P. W. May, and M. N. R. Ashfold, *Diamond Relat. Mater.* **8**, 242 (1999).
- ²³D. G. Goodwin and G. G. Gavillet, *J. Appl. Phys.* **68**, 6393 (1990).
- ²⁴M. E. Coltrin and C. S. Dandy, *J. Appl. Phys.* **74**, 5803 (1993).
- ²⁵I. Schmidt, C. Benndorf, and P. Joeris, *Diamond Relat. Mater.* **4**, 725 (1995).
- ²⁶J. Petherbridge, P. W. May, S. R. J. Pearce, K. N. Rosser, and M. N. R. Ashfold, *Diamond Relat. Mater.* (in press).
- ²⁷F. H. Field and J. L. Franklin, *Electron Impact Phenomena and the Properties of Gaseous Ions* (Academic, New York, 1957).
- ²⁸H. Chatham, D. Hils, R. Robertson, and A. Gallagher, *J. Chem. Phys.* **81**, 1770 (1984).
- ²⁹P. Plessis and P. Marmet, *Can. J. Phys.* **65**, 165 (1986).
- ³⁰Gas Research Institute, Chicago, Illinois, Report GRI-97/0020 (1997).
- ³¹E. Kondoh, T. Ohta, T. Mitomo, and K. Ohtsuka, *J. Appl. Phys.* **73**, 3041 (1993).
- ³²K. A. Snail and C. M. Marks, *Appl. Phys. Lett.* **60**, 3135 (1992).
- ³³H. Maeda, K. Ohtsubo, M. Irie, N. Ohya, K. Kusakabe, and S. Morooka, *J. Mater. Res.* **10**, 3115 (1995).
- ³⁴A. Streitwieser and C. H. Heathcock, *Introduction to Organic Chemistry* (MacMillan, New York, 1981).
- ³⁵J. B. Pedley, R. D. Naylor, and S. P. King, *Thermochemical Data of Organic Compounds* (Chapman and Hall, London, 1986).
- ³⁶S. C. Eaton and M. K. Sunkara, *Diamond Relat. Mater.* **9**, 1320 (2000).
- ³⁷M. W. Chase, *J. Phys. Chem. Ref. Data Monogr.* **9**, 1 (1998).
- ³⁸D. G. Goodwin and J. E. Butler, *Handbook of Industrial Diamonds and Diamond Films* (Marcel Dekker, New York, 1998), p. 541.